

Organisation of mitochondria in living sensory neurons

Vadim N. Dedov, Basil D. Roufogalis*

Department of Pharmacy, University of Sydney, Sydney, NSW 2006, Australia

Received 30 April 1999; received in revised form 15 June 1999

Abstract In this work, we have examined the mitochondrial organisation in living cultured primary dorsal root ganglion (DRG) neurons. Confocal microscopy and the mitochondrial potential-sensitive fluorescent dye 5,5',6,6'-tetrachloro-1,1',3,3'-tetraethylbenzimidazolo carbocyanine iodide (JC-1) were used to visualise intracellular structures with a high and low membrane potential. Three-dimensional reconstruction revealed a mitochondrial organisation featuring separate highly polarised mitochondria, clusters of mitochondria located mainly at the base of neurite hillocks and filamentous mitochondrial structures. Filamentous mitochondria were distributed along the cell body, especially between neurites. A functional integration between mitochondrial structures is proposed.

© 1999 Federation of European Biochemical Societies.

Key words: Sensory neuron; Mitochondrion; Fluorescent probe 5,5',6,6'-tetrachloro-1,1',3,3'-tetraethylbenzimidazolo carbocyanine iodide; Mitochondrial membrane potential

1. Introduction

Our understanding of the structure and organisation of mitochondria primarily comes from transmission electron microscopy developed in the 1950s (for reviews see [1,2]). Classically, mitochondria are described as pleomorphic cytoplasmic structures averaging about 5 µm in length and 100 nm in width. For example, electron microscopy of murine Purkinje cells showed round-shaped and cylindrical mitochondria distributed evenly over the cytoplasm [3]. In several cell types including fibroblasts, mitochondria were found as an extended reticular network [1]. However, a neuronal mitochondrial network has yet to be described.

Amongst mitochondria-specific fluorescent dyes, 5,5',6,6'-tetrachloro-1,1',3,3'-tetraethylbenzimidazolo carbocyanine iodide (JC-1) is the most reliable, reflecting $\Delta\psi$ in living cells [4]. JC-1 exists as a monomer at low concentrations and as aggregates, called J-aggregates, at higher concentrations. JC-1 monomer is excited with a maximum at 490 nm and emits at around 530 nm. Upon aggregation, the fluorescent emission peak shifts to a maximum at 590 nm. As a consequence, mitochondria having a low membrane potential will accumulate low concentrations of JC-1 and will fluoresce in green, in more highly polarised regions within mitochondria, fluorescence will be orange-red. It was estimated that mitochondria with $\Delta\psi$ exceeding 140 mV would form J-aggregates [5].

Here, we use JC-1 fluorescence to reconstruct the three-dimensional organisation of mitochondria in living neurons.

Three types of mitochondrial organisation and shape were found to co-exist in neurons: separate cylindrically shaped mitochondria, filamentous mitochondria and mitochondria organised in clusters.

2. Materials and methods

This study was approved and carried out in accordance with the guidelines of the Animal Ethics Committee of the Sydney University. Dorsal root ganglia (DRG) from neonatal (3–5 days old) Sprague-Dawley rats were incubated in Hanks CMF saline with 0.05% collagenase and 0.25% trypsin for 25 min at 37°C. Individual cells were obtained by trituration with fire-polished Pasteur pipettes of diminishing diameters. Neurons were isolated from the cell suspension in 30% Percoll and plated on collagen-coated coverslips in 24 well plates, then cultured in Neurobasal medium (Gibco) with B27 supplement, 50 ng/ml 2.5 S nerve growth factor (NGF), 2 mM L-glutamine and 100 U/ml penicillin/streptomycin. Cultures were maintained at 37°C with 5% CO₂ for 1–5 days. For video-enhanced phase-contrast microscopy, CCD-72 (DATE) was used with a video-intensifier (Hamamatsu) attached to a Nikon Diaphot inverted microscope fitted with a 40× Fluo (NA 0.85) DL Ph3 objective. All reagents were of analytical grade. JC-1 was obtained from Molecular Probes (Eugene, OR, USA), neurobasal medium with B27 supplement from GIBCO (Gaithersburg, MD, USA), NGF from ICN Biochemicals (Costa Mesa, CA, USA). Other agents were obtained from Sigma (St. Louis, MO, USA).

Neurons on coverslips were incubated with 3 µM JC-1 in physiological solution for 20 min at 37°C. The coverslips were then mounted on a chamber attached to a perfusion system which allows continuous flow of solutions over neurons [6]. Cells were continuously perfused with a physiological solution consisting of 140 mM NaCl, 2 mM CaCl₂, 5 mM KCl, 20 mM HEPES, 10 mM glucose, pH 7.4. Recordings were made on the stage of a Axiophot (Zeiss) up-right microscope equipped with a 40× water immersion objective (NA 0.8) in the Key Centre for Microscopy (University of Sydney). A confocal system MRC-600 (Bio-Rad) with Kr/Ar laser and K1/K2 filter set was used for image acquisition. Photomultipliers and the aperture size were set to produce the brightest images possible against minimal background. A neutral density filter was used to allow 10% transmittance of the laser beam. The fast scan option was used to minimise bleaching and phototoxic effects. Using the 'zoom' option, the image of one single neuron was magnified and individual mitochondria were visualised. Optical sectioning in the Z-plane was performed in 0.54 µm increments. Experiments were performed at room temperature in a darkened room. JC-1 was excited at 490 nm, emission fluorescence was filtered and images were collected at FITC (530 nm) and TRITC (590 nm) channels.

Images were collected using the MRC-600 and COMOS (Bio-Rad) software. Three-dimensional reconstruction was performed using 'Confocal Assistant' (Bio-Rad) software. This software allowed for not only reconstruction of fluorescence images in three dimensions for both 530 and 590 nm images but also to rotate them in parallel. Rotation allowed for visualisation of spatial details that were not revealed by analysing individual images, whereas analysis of red and green fluorescence images in parallel allowed for relative assessment of the mitochondrial membrane potential [5].

3. Results

3.1. Visualisation of mitochondria in living sensory neurons

Fig. 1 represents video-enhanced phase-contrast images of

*Corresponding author. Fax: (61) (2) 9351 4447.

E-mail: basilr@pharm.usyd.edu.au

Abbreviations: DRG, dorsal root ganglia; JC-1, 5,5',6,6'-tetrachloro-1,1',3,3'-tetraethylbenzimidazolo carbocyanine iodide

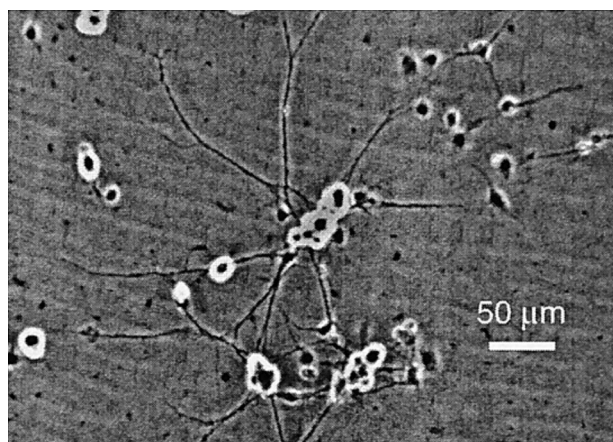


Fig. 1. Phase-contrast video-image showing a DRG neurons culture incubated overnight as described in Section 2.

DRG neurons taken the second day after isolation, revealing typical morphological features, including phase-contrast halo, round shape, a size of about 20 μm in diameter and considerable dendrite outgrowth [7].

Figs. 2–5 are fluorescent images of DRG neurons loaded with JC-1. They represent typical images from three-dimensional reconstructions, which allow for the best view of the mitochondrial structure and organisation (see Section 2). Background staining was faint, but allowed for assessment of the cell shape. The areas not stained with JC-1 (Fig. 1) are likely to be nuclei, which have been shown not to be stained with JC-1 [5].

In all figures, (a) shows red (TRITC) and (b) green (FITC) emission fluorescence. Thus, (a) shows structures with a high $\Delta\varphi$ (greater than -140 mV), whereas (b) shows structures with a low $\Delta\varphi$ potential (smaller than -140 mV) [8].

Ratios between intensities of red and green fluorescence were used to assess $\Delta\varphi$ changes in living central neurons [9]. DRG neurons expressed average ratios of 1.29 ± 0.17 ($n = 16$). Upon addition of mitochondrial uncoupler (2 μM carbonyl cyanide *p*-(trifluoromethoxy) phenylhydrazone), which transports protons through the mitochondrial membrane and dissipates $\Delta\varphi$, ratios decreased to 0.53 ± 0.08 ($n = 16$). It is unlikely that other intracellular organelles except mitochondria are able to accumulate JC-1 in an uncoupler-sensitive manner [5]. Thus, red and green fluorescence presented in Fig. 1 originates from mitochondria. These data also indicate a range of charges between fully charged mitochondria (ratios over one) and fully uncoupled mitochondria (ratios about 0.5), agreeing with data from the literature [9].

When taken over the whole cell, ratio values reflect the average $\Delta\varphi$ of cellular mitochondria. However, values of $\Delta\varphi$ for individual mitochondria may be different [10]. Mitochondria with the greatest $\Delta\varphi$ (-200 mV) emit only at 590 nm, where JC-1 exists only in J-aggregate forms [8]. Such mitochondria are presented in Fig. 5 (C). Less charged mitochondria emit both red and green fluorescence (Fig. 3 (C)).

3.2. Mitochondrial organisation

According to literature available on mitochondrial morphology (see Section 4) and JC-1 staining patterns described for various cell lines [10], including neuronal PC12 cells [11], we expected to see only a uniform distribution of round,

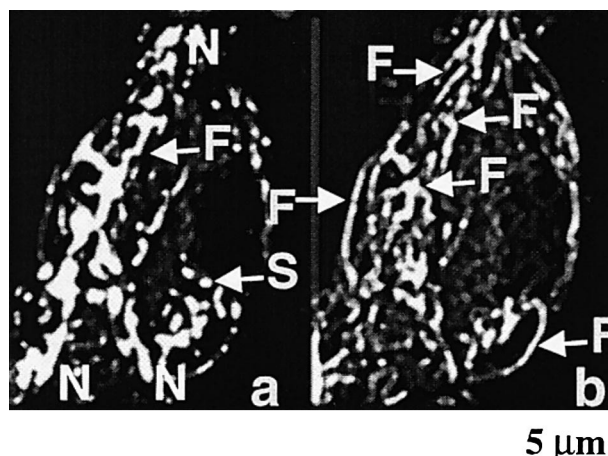


Fig. 2. Images of JC-1 fluorescence reconstructed in three dimensions in DRG neurons (see Section 2). (a) Red fluorescence (TRITC channel), (b) green fluorescence (FITC channel), (N) neurites, (S) separate mitochondria (C) clusters of mitochondria, (F) filamentous mitochondria.

spindle-shaped and/or cylindrical mitochondria over the cytoplasm. However, analysis of three-dimensional reconstructions of JC-1 fluorescence in living neurons showed a mitochondrial organisation with the following features:

- Separate mitochondria (Figs. 2–5 (S)). These mitochondria were visualised better in the red channel (a) and had a size, shape and distribution comparable to those described previously using JC-1 [10]: their size was about 1 μm , they have round and cylindrical shapes and could be found in any part of the cytoplasm. We also observed mitochondria in the proximal part of neurites (all figures, N). Mitochondria were distributed alongside the neurites and had a high $\Delta\varphi$, consistent with what is known from the literature [12,13].
- Clusters of mitochondria (Figs. 3–5 (C)). In the majority of neurons studied, 1–3 clusters of mitochondria were found. In some neurons, separate but closely associated mitochondria could be distinguished (Fig. 4), whereas in others (Figs. 3–5), areas of intensive fluorescence of mitochondrial masses about 5 μm in diameter were seen. In most neurons, clusters of mitochondria were located at the base of the neurite hillock (Figs. 2–5 (N)).

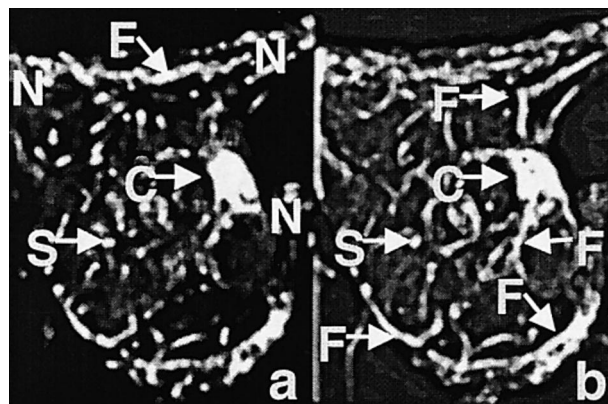


Fig. 3. See the legend of Fig. 2.

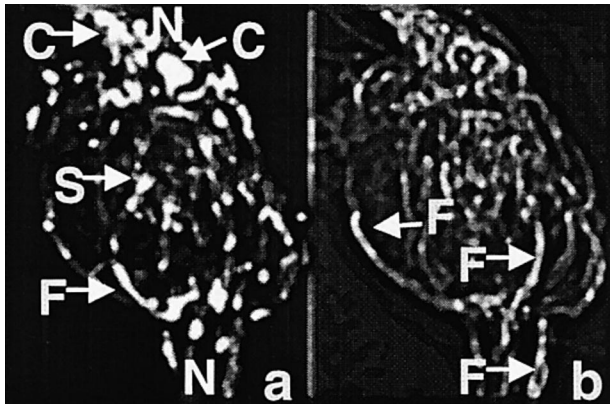


Fig. 4. See the legend of Fig. 2.

- Filamentous mitochondria (Figs. 2–5 (F)). These mitochondria were better distinguished in the green channel (b). Thus, they are less charged than separate mitochondria (see above). In the red channel (a), it was unclear if these are continuous or separate, whereas in the green channel (b), they appeared to be continuous (Figs. 2–5).

4. Discussion

Recently, the fluorescent probe JC-1 was used to study mitochondria in living cells by confocal microscopy [5,10], including primary central neurons [9] and neuronal cell lines [11]. Currently available software allows for three-dimensional reconstructions of cells loaded with fluorescent dyes [14]. Here, we have visualised mitochondria in living neurons with the mitochondria-specific dye JC-1 and analysed their structures by three-dimensional reconstructions of the fluorescent images.

We found that individual mitochondria in neurons can express different staining patterns, reflecting differences in mitochondrial membrane potential. Previously, mitochondrial heterogeneity was also described between cell types [5], between individual mitochondria in cells [10] and in isolated mitochondria [8].

Mitochondrial membrane potential heterogeneity should reflect functional heterogeneity of mitochondria [8,13]. Areas

within the cell with a maximum density of highly charged mitochondria may be considered to reflect regions of the cell with high metabolic activities. For example, in primary central neurons, the dendrite metabolic activity prevails over that in the axons [13]. In DRG neurons, we found clusters of highly charged mitochondria at the base of hillocks. Mitochondria can be transported along axons to provide ATP supply for the growing cone of neurites and clusters of mitochondria may represent a movable pool of mitochondria [15]. Even overnight incubation of neurons is sufficient to cause considerable dendrite outgrowth, at least in some neurons (Fig. 1).

Heterogeneity in the mitochondrial organisation was also found. Mitochondria were represented as separate round mitochondria, mitochondrial clusters and filamentous mitochondria. Filamentous mitochondria were distributed along cell bodies between neurites. Such a mitochondrial organisation provided by filamentous mitochondrial structures may signify a functional connection between the plasma membrane, the pool of separate mitochondria and mitochondrial clusters. Recently, clusters of mitochondria with individual mitochondria connected by intermitochondrial contacts were described for the dorsal column synapses [16].

The concept of a mitochondrial reticulum, filamentous mitochondria and power transmission along mitochondrial membranes was proposed by V.P. Skulachev in the 1980s (see for review [2]). Filamentous mitochondria were found in human fibroblasts, whereas clusters of mitochondria connected by thin filamentous mitochondria were described in rat cardiomyocytes. In both cases, functional connections between mitochondria and lateral proton gradient transmission were suggested [2]. Recently, it was found that mitochondria are excitable organelles capable of generating and conveying electrical and calcium signals [17]. In neurons, mitochondria may be coupled functionally by intracellular Ca^{2+} because neuronal excitation results in intracellular Ca^{2+} transients in the cytoplasm and mitochondria (see for review [18]) and changes of the mitochondrial membrane potential are correlated with intracellular Ca^{2+} transients [19].

Acknowledgements: We thank Dr. G. Cox and Mrs. E. Kable (in the Electron Microscopy Unit) for assistance with the confocal microscopy.

References

- [1] Bereiter-Hahn, J. and Voth, M. (1994) *Microsc. Res. Tech.* 27, 198–219.
- [2] Skulachev, V.P. (1990) *J. Membr. Biol.* 114, 97–112.
- [3] Dunn, M.E., Schilling, K. and Mugnaini, E. (1998) *Anat. Embryol.* 197, 9–29.
- [4] Salvio, S., Ardizzoni, A., Franceschi, C. and Cossarizza, A. (1997) *FEBS Lett.* 411, 77–82.
- [5] Reers, M., Smiley, S.T., Mottola-Hartshorn, C., Chen, A., Lin, M. and Chen, L.B. (1995) *Methods Enzymol.* 260, 406–417.
- [6] Dedov, V.N. and Roufogalis, B.D. (1998) *Neurosci. Lett.* 248, 151–154.
- [7] Lawson, S.N. (1979) *J. Neurocytol.* 8, 275–294.
- [8] Cossarizza, A., Ceccarelli, D. and Masini, A. (1996) *Exp. Cell Res.* 222, 84–94.
- [9] White, R.J. and Reynolds, I.J. (1996) *J. Neurosci.* 16, 5688–5697.
- [10] Smiley, S.T., Reers, M., Mottola-Hartshorn, C., Lin, M., Chen, A., Smith, T.W., Steele Jr., G.D. and Chen, L.B. (1991) *Proc. Natl. Acad. Sci. USA* 88, 3671–3675.
- [11] Wadia, J.S., Chalmers-Redman, R.M.E., Ju, W.J.H., Carlile, G.W., Phillips, J.L., Fraser, A.D. and Tatton, W.G. (1998) *J. Neurosci.* 18, 932–947.

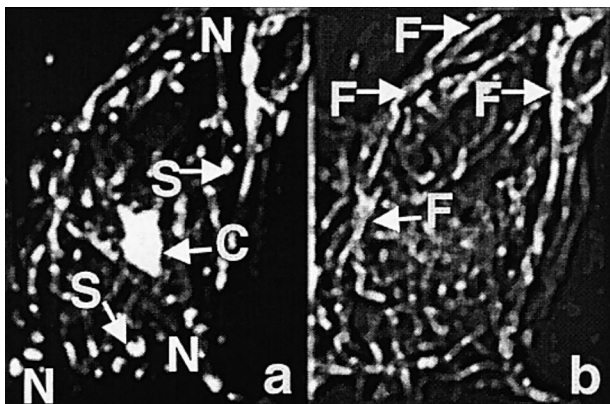


Fig. 5. See the legend of Fig. 2.

- [12] Loew, L.M., Tuft, R.A., Carrington, W. and Fay, F.S. (1993) *Biophys. J.* 65, 2396–2407.
- [13] Overly, C.C., Rieff, H.I. and Hollenbeck, P.J. (1996) *J. Cell Sci.* 109, 971–980.
- [14] Porwol, T., Merten, E., Opitz, N. and Acker, H. (1996) *Acta Anat.* 157, 116–125.
- [15] Morris, R.L. and Hollenbeck, P.J. (1993) *J. Cell Sci.* 104, 917–927.
- [16] Brodin, L., Bakeeva, L. and Shupliakov, O. (1999) *Philos. Trans. R. Soc. Lond. B. Biol. Sci.* 354, 365–372.
- [17] Ichas, F., Jouaville, L.S. and Mazat, J.P. (1997) *Cell* 89, 1145–1153.
- [18] Simpson, P.B. and Russell, J.T. (1998) *Brain Res. Brain Res. Rev.* 26, 72–81.
- [19] Duchen, M.R. (1992) *Biochem. J.* 283, 41–50.